Molecular Mechanism of the Enterococcal Aminoglycoside 6′-*N*-Acetyltransferase′: Role of GNAT-Conserved Residues in the Chemistry of Antibiotic Inactivation†

Kari-ann Draker and Gerard D. Wright*

Antimicrobial Research Centre, Department of Biochemistry, McMaster University, 1200 Main Street West, Hamilton, Ontario L8N 3Z5, Canada

Received September 15, 2003; Revised Manuscript Received November 10, 2003

ABSTRACT: The Gram-positive pathogen *Enterococcus faecium* is intrinsically resistant to aminoglycoside antibiotics due to the presence of a chromosomally encoded aminoglycoside 6′-*N*-acetyltransferase [AAC-(6′)-Ii]. This enzyme is a member of the GCN5-related *N*-acetyltransferase (GNAT) superfamily and is therefore structurally homologous to proteins that catalyze acetyl transfer to diverse acyl-accepting substrates. This study reports the investigation of several potential catalytic residues that are present in the AAC(6′)-Ii active site and also conserved in many GNAT enzymes. Site-directed mutagenesis of Glu72, His74, Leu76, and Tyr147 with characterization of the purified site mutants gave valuable information about the roles of these amino acids in acetyl transfer chemistry. More specifically, steady-state kinetic analysis of protein activity, solvent viscosity effects, pH studies, and antibiotic resistance profiles were all used to assess the roles of Glu72 and His74 as potential active site bases, Tyr147 as a general acid, and the importance of the amide NH group of Leu76 in transition-state stabilization. Taken together, our results indicate that Glu72 is not involved in general base catalysis, but is instead critical for the proper positioning and orientation of aminoglycoside substrates in the active site. Similarly, His74 is also not acting as the active site base, with pH studies revealing that this residue must be protonated for optimal AAC(6′)-Ii activity. Mutation of Tyr147 was found not to affect the chemical step of catalysis, and our results were not consistent with this residue acting as a general acid. Last, the amide NH group of Leu76 is implicated in important interactions with acetyl-CoA and transition-state stabilization. In summary, the work described here provides important information regarding the molecular mechanism of AAC(6′)-Ii catalysis that allows us to contrast our findings with those of other GNAT proteins and to demonstrate that these enzymes use a variety of chemical mechanisms to accelerate acyl transfer.

Bacterial resistance to the aminoglycoside−aminocyclitol antibiotics is most commonly due to the action of *O*-phosphotransferases (APHs),[1] *O*-nucleotidylyltransferases (ANTs), and *N*-acetyltransferases (AACs), which modify various hydroxyl or amino functionalities on the drug (*1*, *2*). Antibiotic modification by these aminoglycoside-modifying enzymes (AMEs) decreases the affinity of the antibiotic for its 30S ribosomal subunit target (*3*), resulting in microbial resistance and complications in the clinical treatment of infections caused by both Gram-positive and Gram-negative bacteria. In Gram-positive enterococci in particular, high-level resistance to gentamicin (*4*) as well as lower-level resistance to several other aminoglycosides (*5*) renders routine β-lactam/aminoglycoside therapy ineffective. This failure of commonplace treatments increases the reliance on other classes of drugs such as the glycopeptides, resulting in an additional clinical problem in the form of vancomycin resistant enterococci (VRE) and a disturbing trend of bacterial multidrug resistance (*6*, *7*).

A prevalent form of modification conferring aminoglycoside resistance in bacteria is 6′-N-acetylation, with two such enzymes responsible for antibiotic inactivation in Gram-positive enterococci (*2*, *8*). In *Enterococcus faecalis*, high-level aminoglycoside resistance is often due to the plasmid-mediated expression of the AAC(6′)−APH(2″) bifunctional enzyme, which both acetylates and phosphorylates various aminoglycosides (*9*). In *E. faecium*, intrinsic resistance is mediated by expression of the chromosomally encoded *aac-(6′)-Ii* gene, conferring low-level resistance to the 4,5- and 4,6-disubstituted deoxystreptamine classes of aminoglycosides (*10*). *In vitro* characterization of purified AAC(6′)-Ii revealed its broad substrate specificity and defined the kinetics of acetyl transfer to be suboptimal for a detoxification enzyme, with fairly low specificity constants (k_{cat}/K_m values) on the order of 10^4 M^{-1} s^{-1} and poor correlation of this specificity with the minimum inhibitory concentration (MIC) (*11*). More recent studies have shown that AAC(6′)-Ii follows an ordered Bi-Bi reaction mechanism similar to those of numerous other *N*-acetyltransferases, in which acetyl-CoA binds first to the enzyme followed by aminogly-

† This work was supported by Canadian Institutes of Health Research Grant MT-13536 and a Canada Research Chair in Antibiotic Biochemistry to G.D.W.

* To whom correspondence should be addressed. Telephone: (905) 525-9140, ext. 22454. Fax: (905) 522-9033. E-mail: wrightge@mcmaster.ca.

[1] Abbreviations: APH, aminoglycoside phosphotransferase; ANT, aminoglycoside nucleotidylyltransferase; AME, aminoglycoside-modifying enzyme; VRE, vancomycin resistant enterococci; GNAT, GCN5-related *N*-acetyltransferase; AANAT, arylalkylamine *N*-acetyltransferase; GNA1, glucosamine-6-phosphate acetyltransferase; HAT, histone acetyltransferase.

10.1021/bi035667n CCC: $27.50
Published on Web 12/20/2003

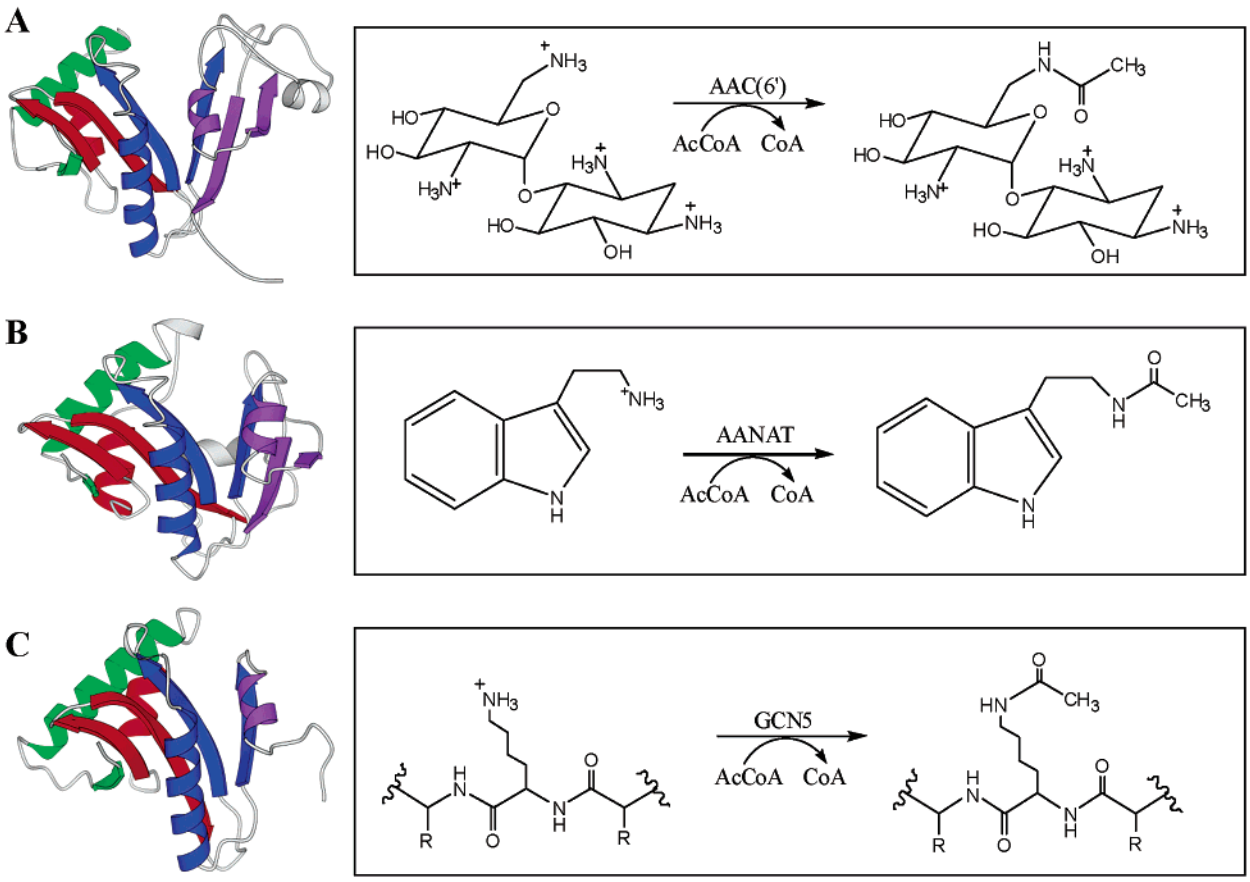

FIGURE 1: Structures of three representative classes of GNAT enzymes (left) and the diverse acetyltransferase reactions they catalyze (right). (A) Typical kanamycin modification by a bacterial aminoglycoside 6′-*N*-acetyltransferase, like AAC(6′)-Ii (shown) (*13*). (B) Eukaryotic arylalkylamine *N*-acetyltransferases (AANATs) catalyze the acetylation of small molecules such as serotonin. Shown is AANAT from sheep (*18*). (C) The N-acetylation of histones at specific lysine residues is accomplished by HAT enzymes, like the tetrahymena GCN5 protein that is shown (*23*). Structures of each of the represented proteins were generated using MOLSCRIPT (*37*) and Raster3D (*38*), with GNAT sequence motifs A−D colored blue, purple, green, and red, respectively.

coside to form a productive ternary complex (*12*). Solvent viscosity and isotope effects also revealed that diffusion-controlled processes and not the chemical step govern the rate of AAC(6′)-Ii acetyl transfer (*12*).

The crystal structure of AAC(6′)-Ii in complex with acetyl-CoA (*13*) identified this resistance enzyme as a member of the large GCN5-related *N*-acetyltransferase (GNAT) superfamily, which includes a diverse group of enzymes from both prokaryotes and eukaryotes. Originally based on primary sequence data which identified four sequence motifs common to *N*-acetyltransferases, early structural determinations of two GNAT members first revealed the remarkable structural homology among superfamily members despite the lack of extensive primary sequence homology (*14*, *15*). The subsequent structural determination of the AAC(6′)-Ii·acetyl-CoA binary complex helped to further define the four conserved structural motifs and their role in acetyl-CoA binding, as well as to characterize AAC(6′)-Ii as both a structural and functional homologue of eukaryotic histone acetyltransferases (HATs) (*13*). Numerous GNAT crystal structures are now available that exemplify both the structural similarities among superfamily members and the diverse specificity of these enzymes for acyl-accepting substrates, such as aminoglycosides and other sugars (*13*, *14*, *16*, *17*), small molecules such as serotonin (*18*, *19*), and histones and other proteins (*15*, *20*−*25*) (Figure 1).

To date, crystal structures of three aminoglycoside *N*-acetyltransferases representing the 3-, 2′-, and 6′-regiospecificities of drug modification have been determined (*13*, *14*, *17*). A structure-based sequence alignment of these AACs with other homologues in the GNAT superfamily provides information regarding the residues conserved within structural motifs A−D (Figure 2). In addition to the numerous nonpolar residues that are important for the GNAT structural fold (*26*), several active site amino acids that could play a catalytic role are also structurally aligned in highly conserved motifs A and B (Figure 2). In particular, AAC(6′)-Ii residues Glu72, His74, Leu76, and Tyr147 align well with chemically similar residues from several GNATs (Figure 2) and have the potential to play a role in general acid/base catalysis or transition-state stabilization that is typical for an acetyl transfer reaction (Figure 3A).

This study concentrates on these potential catalytic residues that line the AAC(6′)-Ii active site, represented in Figure 3B. Amino acids Glu72, His74, and Leu76 are found on β-strand 4 (motif A), which contains the GNAT-conserved β-bulge and makes the majority of contacts with acetyl-CoA (*13*, *26*). Tyr147 is part of α-helix 5 (motif B), which also interacts with the bound cofactor in the AAC(6′)-Ii crystal structure. More specifically, Glu72 is in the proximity of the substrate acetyl moiety and may act as a general base by deprotonating the incoming 6′-amino group of the

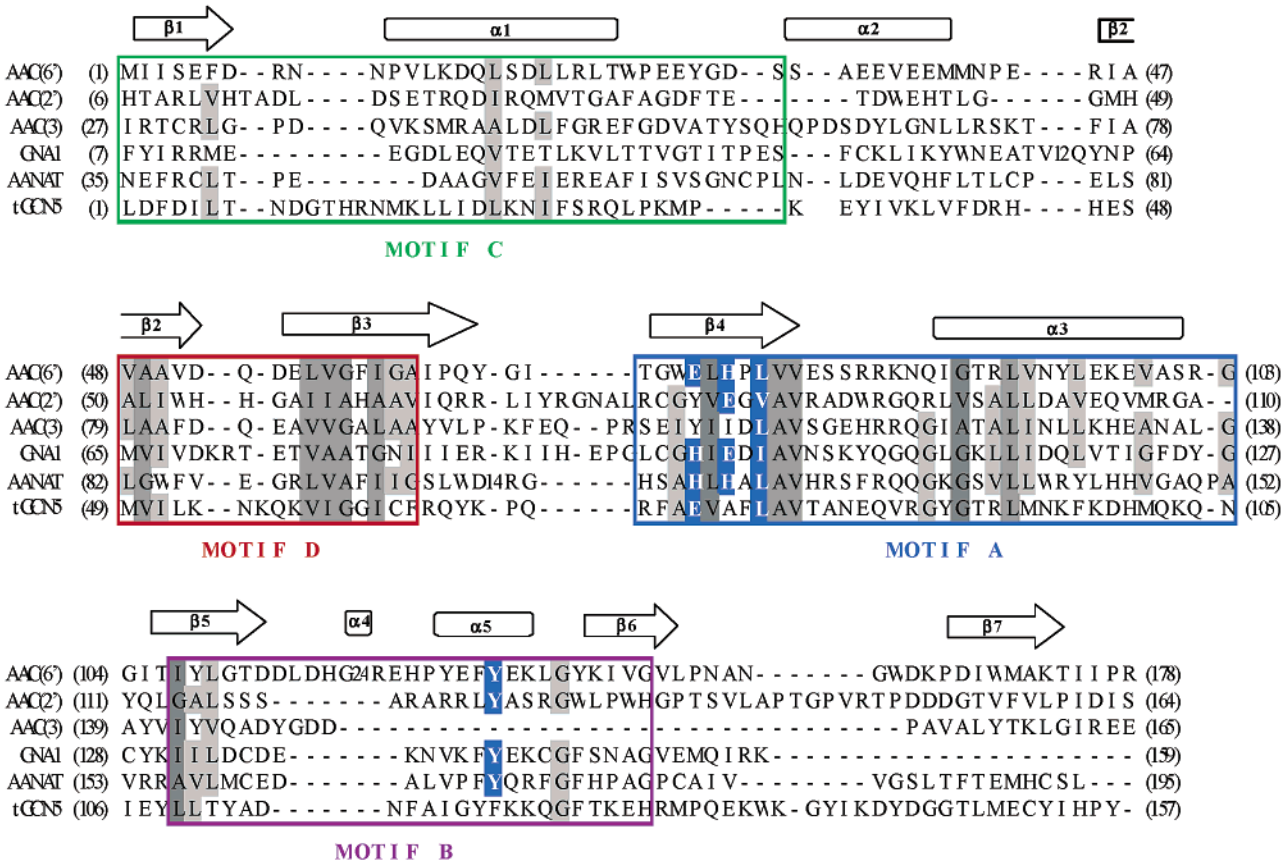

FIGURE 2: Structure-based sequence alignment of representative members of the GNAT superfamily. Included (from top) are primary sequences of the aminoglycoside acetyltransferases AAC(6′)-Ii (*13*), AAC(3)-Ia (*14*), and AAC(2′)-Ic (*17*), as well as the sugar transferase GNA1 (*16*), AANAT (*18*), and tGCN5 (*23*). The alignment was generated using the Vector Alignment Search Tool (VAST) algorithm (*39*, *40*). Nonpolar residues important for the GNAT structural fold are boxed in dark gray (conserved) or light gray (semi-conserved). Boxed in blue with white font are potential catalytic residues that are conserved among some members, including AAC(6′)-Ii residues Glu72, His74, Leu76, and Tyr147. GNAT structural motifs A−D are outlined with the same color-coding used in Figure 1. Secondary structural elements for AAC(6′)-Ii are shown above the primary sequence.

aminoglycoside. His74 could behave as either a general acid or base in drug modification. The backbone NH group of Leu76 may also be critical for AAC(6′)-Ii catalysis, as this main chain element is in the proximity of the carbonyl oxygen of acetyl-CoA (Figure 3B) and equivalent residues have been repeatedly implicated in transition-state stabilization for several GNATs (*17*, *18*, *23*, *24*). Finally, the hydroxyl group of Tyr147 interacts with the sulfur atom of acetyl-CoA (Figure 3B) and thus has the potential to act as a general acid in acetyl transfer by reprotonating the CoA leaving group. Interestingly, several amino acids from various GNATs that structurally align with the aforementioned AAC(6′)-Ii residues have already been shown to play critical roles in reaction chemistry. These include Glu173 of yeast GCN5 [aligns with Glu72 of AAC(6′)-Ii], which has been shown by mutagenesis and kinetic analysis to act as the general base in histone acetylation (*27*). Recent studies on AANAT have shown that His122 [aligns with His74 of AAC(6′)-Ii (Figure 2)] acts as a remote general base in serotonin acetylation, with Tyr168 [aligns with Tyr147 of AAC(6′)-Ii (Figure 2)] behaving as the general acid (*28*).

This report describes the characterization of AAC(6′)-Ii site mutants Glu72Ala, His74Ala, Leu76Ala, Leu76Pro, Tyr147Ala, and Tyr147Phe. Kinetic analysis of mutant enzyme activity was followed by solvent viscosity studies to determine whether any of the amino acid substitutions resulted in a protein impaired at the chemical step of acetyl transfer. Additional studies on the pH dependence of wild-type and His74Ala activity identified ionizable groups that are important for catalysis and further defined the chemical mechanism of AAC(6′)-Ii. Finally, the impact of each amino acid substitution on AAC(6′)-Ii drug acetylation *in vivo* was assessed by MIC determinations of select aminoglycoside antibiotics. The goal of this work is to elucidate the molecular mechanism of aminoglycoside inactivation by this enzyme, which will no doubt be useful in the identification and/or design of AAC(6′)-Ii specific inhibitors in the future. In addition, an understanding of the chemical mechanisms of GNAT enzymes and how they differ may shed light on the broad specificities displayed for acyl-accepting substrates and on the evolution of these *N*-acyltransferases as a superfamily.

MATERIALS AND METHODS

General. Aminoglycosides and 4,4′-dithiodipyridine (DTDP) were from Sigma Chemical Co. (St. Louis, MO). Neamine was the kind gift of S. Mobashery at the Institute for Drug Design, Departments of Chemistry, Pharmacology, and Biochemistry and Molecular Biology, Wayne State University, Detroit, MI. Acetyl-CoA was from Amersham Pharmacia, and [1-^{14}C]acetyl-CoA (specific activity of 65 mCi/mmol) was from ICN Radiochemicals (Costa Mesa, CA). Mutagenic oligonucleotide primers were synthesized at the Central Facility of the Institute for Molecular Biology and Biotechnology, McMaster University.

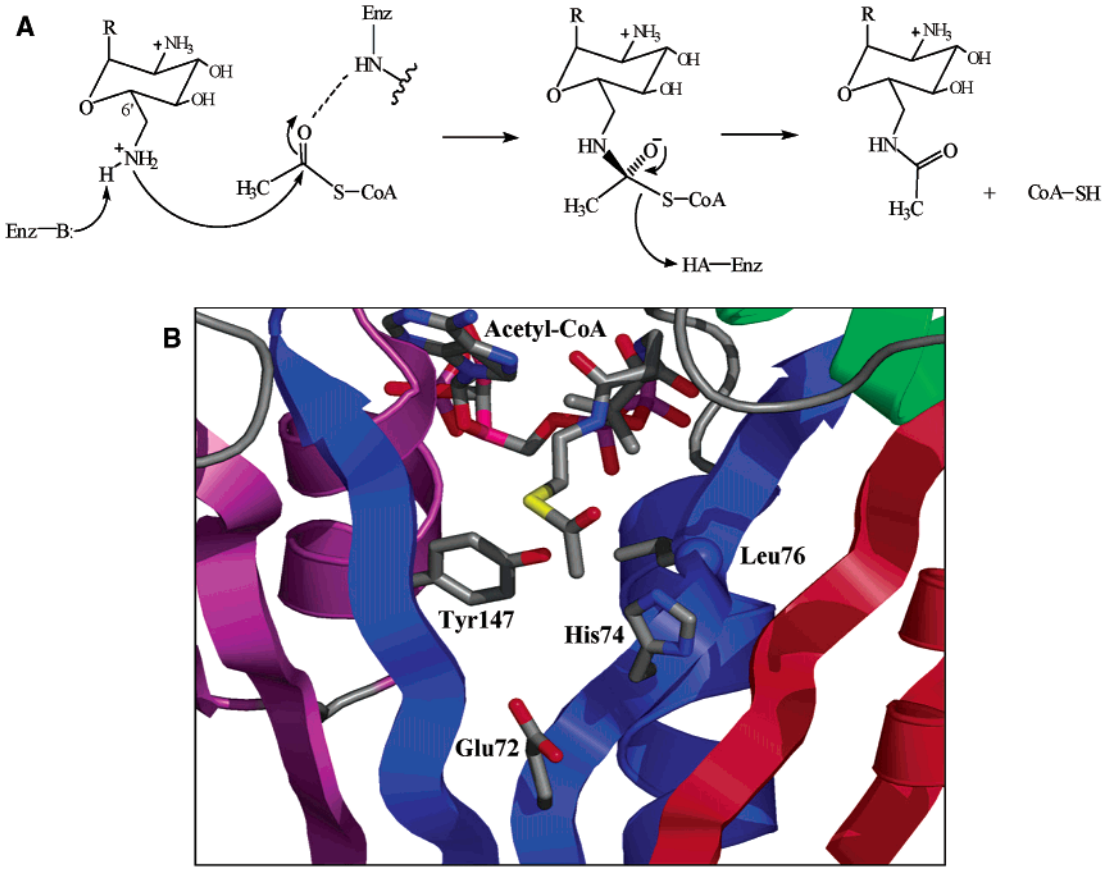

FIGURE 3: Proposed reaction pathway for AAC(6′)-Ii-catalyzed acetyl transfer and potential catalytic residues lining the active site. (A) Probable mechanism of aminoglycoside acetylation by AAC(6′)-Ii, showing nucleophilic attack of the carbonyl carbon of acetyl-CoA by the deprotonated 6′-amino group of an aminoglycoside (right) and formation of a tetrahedral-like transition state (middle). Possible general acid/base catalysis and transition-state stabilization by the enzyme are also shown. (B) AAC(6′)-Ii active site with bound acetyl-CoA and nearby amino acids Glu72, His74, Leu76, and Tyr147. The potential roles of these residues are discussed throughout the text. The sulfur atom of acetyl-CoA is colored yellow, and the amide N of Leu76 is represented as a blue sphere. Secondary structure that is part of a conserved motif is colored blue (motif A), purple (motif B), green (motif C), or red (motif D).

Table 1: Mutagenic Oligonucleotides Used in This Study

mutation	oligonucleotide sequence[a]
Glu72Ala	5′-ggtatcacaggttgggcattgcatccattag-3′
Glu72Gln	5′-ggtatcacaggttggcaattgcatccattag-3′
Glu72Asp	5′-ggtatcacaggttgggatttgcatccattag-3′
His74Ala	5′-ggttgggaattggctccattagttgtagaaagc-3′
Leu76Ala	5′-gggaattgcatccagcagttgtagaaagctc-3′
Leu76Pro	5′-gggaattgcatccaccagttgtagaaagctc-3′
Tyr147Ala	5′-ggacatccgtatgagttcgctgaaaaattagg-3′
Tyr147Phe	5′-ggacatccgtatgagttctttgaaaaattagg-3′

[a] Underlined bases denote the codon change used to generate the desired amino acid substitution.

Site-Directed Mutagenesis of AAC(6′)-Ii. To investigate the roles of Glu72, His74, Leu76, and Tyr147 in acetyl transfer, eight site mutants were generated with the QuikChange site-directed mutagenesis protocol (Stratagene, La Jolla, CA) using the appropriate mutagenic oligonucleotide primer (Table 1) and its reverse complement. The wild-type *aac(6′)-Ii* gene cloned into pET22b(+) (Novagen, Madison, WI) (*12*) was used as template DNA in all PCR amplifications. The presence of the desired mutation in all mutant *aac(6′)-Ii* genes as well as the absence of adventitious mutations was confirmed by complete gene sequencing at the Central Facility of the Institute for Molecular Biology and Biotechnology, McMaster University. All expression constructs were used to transform *Escherichia coli* BL21-(DE3) competent cells for subsequent enzyme overexpression and purification.

Purification of Site Mutants. Wild-type and mutant AAC-(6′)-Ii proteins were overexpressed and purified by the three-step column chromatography procedure previously described (*11*). Exceptions were the Glu72Gln and Glu72Asp mutants, which were overexpressed following induction with IPTG at 16 °C overnight. This was done to obtain a reasonable quantity of soluble protein after initial attempts using wild-type procedures were unsuccessful.

Partial Proteolysis of Mutant AAC(6′)-Ii Proteins. Incubation of wild-type AAC(6′)-Ii with subtilisin results in a reproducible pattern of proteolysis as visualized by sodium dodecyl sulfate−polyacrylamide gel electrophoresis (SDS−PAGE). In addition, AAC(6′)-Ii is almost completely protected from proteolysis in the presence of acetyl-CoA, with bound aminoglycoside offering less protection (see the Supporting Information). The susceptibility of mutant AAC-(6′)-Ii proteins to subtilisin was therefore investigated for confirmation that the introduced mutations did not perturb the overall tertiary structure of the proteins, as assessed by visual comparison with wild-type digestion patterns.

Steady-State Kinetic Analysis. Aminoglycoside-dependent acetyltransferase activity was monitored during protein purification and steady-state kinetic studies by *in situ* titration of free coenzyme A with 4,4′-dithiodipyridine (DTDP) as

described previously (*11*, *29*). Assay conditions for the kinetic analysis of mutant AAC(6′)-Ii enzymes were similar to those described for the wild-type protein (*11*), but scaled down to a final volume of 250 μL to monitor reactions in microtiter plate format using a Molecular Devices SpectraMAX Plus spectrophotometer. Initial rates were fit to eq 1 describing Michaelis−Menten kinetics

$$v = k_{cat}E_t[S]/(K_m + [S]) \quad (1)$$

or eq 2

$$v = k_{cat}E_t[S]/[(K_m + [S])(1 + [S]/K_i)] \quad (2)$$

when substrate inhibition was detected, using Grafit 4.0 software (*30*). Peptide acetylation activities of wild-type and Glu72Ala proteins were compared using the modified phosphocellulose binding assay and the model peptide substrate poly-L-Lys as described previously (*13*). Reactions were allowed to proceed for 45 min, and mixtures contained varying concentrations of poly-L-Lys, 0.1 μCi of [1-^{14}C]-acetyl-CoA (160 μM), and ca. 25 pmol of enzyme in 25 mM HEPES (pH 7.5) and 2 mM EDTA.

Sucrose Viscosity Studies on AAC(6′)-Ii Mutants. The rate of acetyl transfer for wild-type AAC(6′)-Ii is largely governed by CoA product release, as recently shown by solvent viscosity effects determined using the microviscosogen sucrose (*12*). Viscosity studies were employed here to assess whether any of the amino acid substitutions under investigation affected the chemical step and therefore altered the rate-limiting segment(s) of the reaction from product release to acetyl transfer chemistry. In such a case, we would not expect changes in enzymatic rates with increasing solvent viscosity. Viscosity studies with Glu72Ala, His74Ala, Leu76Ala, Leu76Pro, Tyr147Ala, and Tyr147Phe site mutants were carried out using the microviscosogen sucrose (from 0 to 30%) and ribostamycin as the varied substrate as described previously (*12*). Initial rate data were fit by nonlinear least squares to eq 1 using Grafit 4.0 software (*30*). Values reported in Table 3 are the slopes of plots from either k_{cat}^0/k_{cat} or $(k_{cat}/K_m^0)/(k_{cat}/K_m)$ versus the relative viscosity of the sucrose-containing solution for each mutant.

Dependence of pH on AAC(6′)-Ii Activity. pH studies on the wild-type enzyme were performed to generate a profile of enzyme activity as a function of pH. Acetyl transfer activity was monitored from pH 5.5 to 9.0 every 0.5 pH unit using overlapping 50 mM buffers of MES (pH 5.5−7.0), HEPES (pH 7.0−8.0), or TAPS (pH 8.0−9.0). The resulting kinetic data were fit to the eq 1 to obtain the first- and second-order kinetic parameters, k_{cat} and k_{cat}/K_m, respectively. Profiles were generated by plotting log k_{cat} or log k_{cat}/K_m as a function of pH and relevant pK values identified by a fit of the data to global equations of best fit using the Enzyme Kinetics Module of Sigma Plot software (*31*). The wild-type AAC(6′)-Ii pH profile fit best to eq 3 describing a single pK_a value

$$\log v = \log[C/(1 + K_a/H)] \quad (3)$$

where v is either the k_{cat} or k_{cat}/K_m rate constant, C represents the pH-independent value, K_a is the acid equilibrium constant, and H is the proton concentration. Similar studies on the His74Ala mutant were performed as described above for the wild-type enzyme.

MIC Determinations. MICs of kanamycin A and neomycin were determined using the serial dilution method in liquid culture and microtiter plate format according to standard

Table 2: Steady-State Kinetic Parameters for Wild-Type and Mutant AAC(6′)-Ii Proteins[a]

substrate	K_m (μM)	k_{cat} (s^{-1})	k_{cat}/K_m (M^{-1} s^{-1})	$[k_{cat}/K_{m(WT)}]/[k_{cat}/K_{m(MUT)}]$
		Wild Type[b]		
acetyl-CoA	23.5 ± 3.7	0.40 ± 0.02	1.7×10^4	
neamine	5.8 ± 1.0	0.42 ± 0.02	7.2×10^4	
kanamycin A	19.9 ± 8.8	0.82 ± 0.21	4.6×10^4	
tobramycin	22.0 ± 5.6	1.1 ± 0.20	5.1×10^4	
amikacin	13.1 ± 2.1	0.11 ± 0.01	8.1×10^3	
neomycin	5.3 ± 0.6	0.20 ± 0.00	3.9×10^4	
ribostamycin	9.1 ± 2.0	0.34 ± 0.22	3.7×10^4	
		Glu72Ala		
acetyl-CoA	154 ± 39	0.99 ± 0.15	6.4×10^3	2.7
neamine	482 ± 49	0.44 ± 0.01	9.1×10^2	79
kanamycin A	3490 ± 512	0.55 ± 0.03	1.6×10^2	290
tobramycin	1150 ± 304	1.1 ± 0.20	9.6×10^2	53
amikacin	380 ± 51	0.05 ± 0.00	1.3×10^2	62
neomycin	29.0 ± 4.2	1.1 ± 0.07	3.8×10^4	1.0
ribostamycin	301 ± 43	0.35 ± 0.02	1.2×10^3	31
		His74Ala		
acetyl-CoA	7.3 ± 0.8	0.18 ± 0.00	2.5×10^4	0.7
neamine	43.2 ± 9.0	0.15 ± 0.02	3.5×10^3	21
kanamycin A	14.4 ± 2.9	0.05 ± 0.00	3.3×10^3	14
tobramycin	36.9 ± 3.6	0.30 ± 0.01	8.2×10^3	6.2
amikacin	58.2 ± 4.8	0.04 ± 0.00	7.1×10^2	11
neomycin	18.2 ± 3.2	0.19 ± 0.01	1.0×10^4	3.9
ribostamycin	38.1 ± 3.9	0.23 ± 0.01	6.0×10^3	6.2
		Leu76Ala		
acetyl-CoA	3.3 ± 0.6	0.23 ± 0.01	6.9×10^4	0.3
neamine	22.4 ± 5.6	0.38 ± 0.01	1.7×10^4	4.2
kanamycin A	25.7 ± 2.6	0.27 ± 0.01	1.1×10^4	4.2
tobramycin	62 ± 12	0.89 ± 0.14	1.4×10^4	3.6
amikacin	11.4 ± 2.1	0.03 ± 0.00	2.5×10^3	3.2
neomycin	19.0 ± 3.0	0.16 ± 0.01	8.4×10^3	4.6
ribostamycin	21.4 ± 1.0	0.15 ± 0.00	7.0×10^3	5.3
		Leu76Pro		
acetyl-CoA	48.9 ± 9.9	0.06 ± 0.00	1.2×10^3	14
neamine	68.2 ± 8.8	0.002 ± 0.000	3.1×10	2300
kanamycin A	no activity[c]			
tobramycin	146 ± 23	0.01 ± 0.00	3.8×10	1300
amikacin	no activity			
neomycin	57.3 ± 5.4	0.04 ± 0.00	6.5×10^2	46
ribostamycin	107 ± 16	0.01 ± 0.00	7.7×10	480
		Tyr147Ala		
acetyl-CoA	4.7 ± 0.8	0.01 ± 0.00	1.6×10^3	11
neamine	169 ± 20	0.004 ± 0.00	2.2×10	3300
kanamycin A	110 ± 41	0.01 ± 0.00	5.6×10	820
tobramycin	147 ± 22	0.004 ± 0.001	2.6×10	1960
amikacin	no activity			
neomycin	38.6 ± 8.8	0.001 ± 0.000	3.6×10	1080
ribostamycin	109 ± 16	0.02 ± 0.00	1.5×10^2	250
		Tyr147Phe		
acetyl-CoA	4.1 ± 0.8	0.07 ± 0.00	1.8×10^4	0.9
neamine	150 ± 24	0.05 ± 0.00	3.2×10^2	2250
kanamycin A	340 ± 14	0.03 ± 0.01	1.0×10^2	460
tobramycin	136 ± 19	0.10 ± 0.00	7.1×10^2	72
amikacin	2190 ± 600	0.003 ± 0.000	1.2	6750
neomycin	55.3 ± 20.8	0.07 ± 0.01	1.3×10^3	30
ribostamycin	306 ± 89	0.12 ± 0.01	4.0×10^2	93

[a] Reactions were carried out at 37 °C in 25 mM MES (pH 6.0) and 1 mM EDTA. [b] Kinetic parameters for wild-type AAC(6′)-Ii are reproduced from ref *11*. [c] No measurable activity observed for up to 3 nmol of protein added per reaction.

Table 3: Solvent Viscosity Effects on Wild-Type and Mutant AAC(6′)-Ii Activities[a]

protein	$(k_{cat}^0/k_{cat})^{\eta}$ [b]	$[(k_{cat}/K_b^0)/(k_{cat}/K_b)]^{\eta}$	catalytic mutant[c]
wild type[d]	0.52	0.72	no
Glu72Ala	0.04	0.02	yes
His74Ala	0.21	−0.03	yes
Leu76Ala	0.61	0.70	no
Leu76Pro	0.35	0.07	yes
Tyr147Ala	0.28	0.45	no
Tyr147Phe	0.54	0.60	no

[a] Reported sucrose viscosity effects are for k_{cat} and k_{cat}/K_b with ribostamycin with varied aminoglycoside and saturating concentrations of acetyl-CoA. [b] The reported values are the slopes of plots for k_{cat}^0/k_{cat} or $(k_{cat}/K_b^0)/(k_{cat}/K_b)$ vs the relative viscosity of the solution. [c] AAC(6′)-Ii proteins with an amino acid substitution that caused the chemical step of acetyl transfer to become rate-limiting was considered a catalytic mutant. [d] Reproduced from ref *12*.

NCCLS guidelines (*32*). The MIC was defined in this study as the lowest concentration of an aminoglycoside antibiotic to completely inhibit growth of *E. coli* BL21(DE3) cells expressing wild-type or mutant AAC(6′)-Ii proteins. *E. coli* BL21(DE3) cells containing pET22b(+) or no plasmid DNA served as MIC controls. Western blot analysis of the AAC(6′)-Ii protein from bacterial lysates confirmed that expression levels of the wild type and the various site mutants were comparable.

RESULTS AND DISCUSSION

Purification and Stability of AAC(6′)-Ii Site Mutants. AAC(6′)-Ii mutants Glu72Ala, His74Ala, Leu76Ala, Leu76Pro, Tyr147Ala, and Tyr147Phe were successfully overexpressed and purified using wild-type procedures, indicating that these proteins maintained the general properties of the native protein. In addition, partial proteolysis patterns for these mutants were identical to that of native AAC(6′)-Ii, providing good evidence that the site mutations did not perturb the overall fold of the enzymes. The Glu72Gln and Glu72Asp mutants, which required lower overexpression temperatures for us to obtain soluble protein, were found to have an increased protease susceptibility and different proteolytic pattern compared to those of wild type, revealing that these proteins did not have the same structural stability as the native enzyme. As a result, only the substitution of Glu72 with Ala was characterized in this study.

Steady-State Kinetic Analysis of AAC(6′)-Ii Site Mutants. Recent work on wild-type AAC(6′)-Ii has shown that the apparent affinity (K_m) of both acetyl-CoA and aminoglycoside for the enzyme approximates the dissociation constant (K_d) for these substrates (Supporting Information and ref *12*). This allows us to directly correlate changes in substrate K_m values for the site mutants as changes in binding affinity. Since we also know that the rate of acetyl transfer by AAC(6′)-Ii is largely governed by product (CoA) release and is reflected in k_{cat} values, changes in catalytic efficiency (k_{cat}/K_m) as well as solvent viscosity effects were used to assess changes in the chemical steps for the various site mutants. The sucrose viscosity studies in particular were found to complement our steady-state kinetic analysis of each site mutant, as we could now assess whether each protein was catalytically impaired at the chemical steps as a result of the introduced mutation. Our results are discussed below for each site mutant with steady-state kinetic results included in Table 2 and solvent viscosity effects presented in Table 3.

Role of Glu72. The mutation of Glu72 to Ala caused a notable reduction in affinity for both the 4,5- and 4,6-disubstituted classes of aminoglycosides, with the largest changes being an 83-fold decrease in the affinity for the minimal substrate neamine and a 175-fold reduction in K_m for kanamycin A (Table 2). Little change in the rate of substrate turnover was observed for any of the aminoglycosides that were tested, with the exception of a 5-fold increase in k_{cat} for neomycin acetylation. Reductions in specificity constants (k_{cat}/K_m) for this mutant were largely a result of the decrease in protein affinity for aminoglycoside substrates, with the efficiency of neamine acetylation reduced by almost 80-fold and the specificity for kanamycin A decreased by 290-fold (Table 2). Sucrose viscosity studies revealed that this mutant was likely impaired at the chemical step of acetyl transfer, as evidenced by the lack of an effect on both k_{cat} and k_{cat}/K_b in response to increasing solvent viscosity (Table 3). Since AAC(6′)-Ii can also modify the model substrate poly-L-lysine (*13*), kinetic parameters were determined for the Glu72Ala mutant using this peptide and revealed no significant change in this activity compared to that of the wild type (1.25-fold change in k_{cat}/K_m).

Taken together, these kinetic results support a role for Glu72 in aminoglycoside recognition and are not consistent with this residue acting as a general base in antibiotic or peptide acetylation. Our results instead suggest that the carboxylate moiety of Glu72 may be interacting, either directly or indirectly, with a common aminoglycoside functional group on the 6-aminohexose or the aminocyclitol ring. The fact that the apparent affinity of AAC(6′)-Ii for the peptide substrate poly-L-Lys was not affected by this mutation provides additional support that this residue interacts specifically with aminoglycoside. Our sucrose viscosity results also imply that Glu72, in addition to its role in aminoglycoside recognition, may be critical for the proper positioning and orientation of this substrate in the AAC(6′)-Ii active site for efficient acetyl transfer to occur. To date, we have mutated and characterized several other acidic residues lining the AAC(6′)-Ii active site, including Glu28, Glu39, Asp112, and Asp168, with no implication of any of these amino acids acting in a general base capacity (results not shown). The possibility remains that an amino acid distant from the active site may serve as a remote general base or, alternatively, that the environment of the AAC(6′)-Ii active site may be such that the aminoglycoside amine is only partially protonated and a general base is therefore not required.

Dependence of the pH of AAC(6′)-Ii Activity and the Role of His74. pH studies on the wild-type enzyme were performed to identify enzyme ionizable groups that are relevant to the acetyl transfer mechanism. As we now know through viscosity studies and solvent isotope effects that substrate turnover, or k_{cat}, is largely governed by a diffusion-controlled process and not the chemical step (*12*), we have concentrated on catalytic efficiency, or k_{cat}/K_m values, in our analysis. In addition, since AAC(6′)-Ii follows an ordered Bi-Bi kinetic mechanism with aminoglycoside being the second substrate added in the formation of a productive ternary complex, changes in k_{cat}/K_b were analyzed to identify ionizable groups and protonation states relevant to both substrate binding and

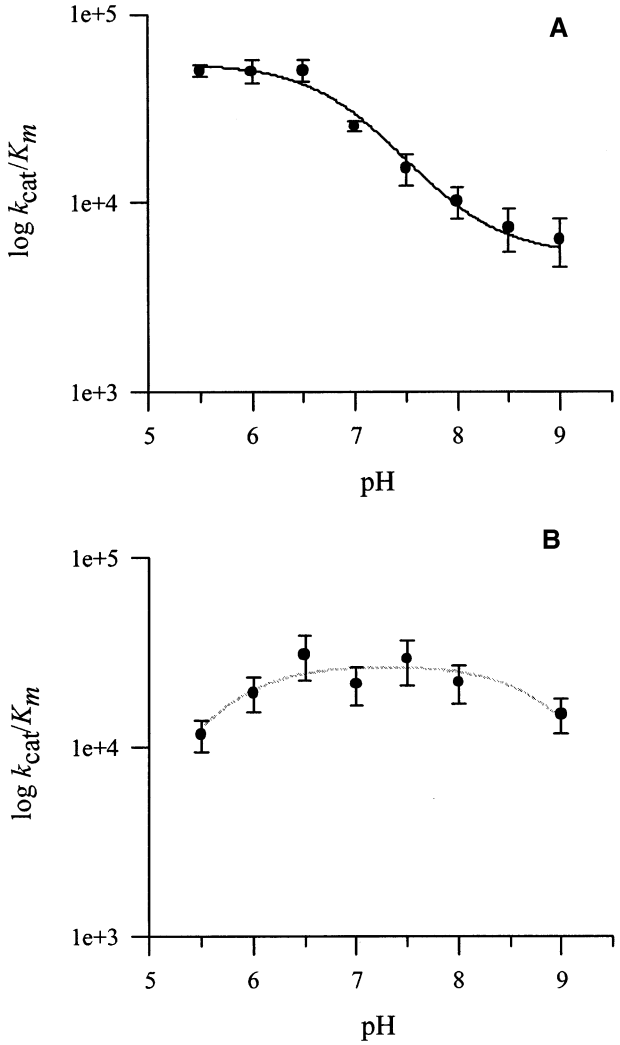

FIGURE 4: pH profiles of wild-type AAC(6′)-Ii (A) and His74Ala (B) activity as a function of pH. Shown are plots of log(k_{cat}/K_b) vs pH, which ranged from 5.5 to 9.0 using 50 mM MES, HEPES, and TAPS buffers as described in Materials and Methods. Enzyme activity was measured with ribostamycin aminoglycoside as the variable substrate and saturating concentrations of acetyl-CoA. A single pK_a of 6.9 ± 0.1 was identified for the wild-type protein on the basis of the best fit of the generated data to eq 3. No relevant pK value was determined from the His74Ala pH profile based on the collected data.

catalysis (*33*). The results of our pH studies with wild-type AAC(6′)-Ii indicate that an ionizable group with a pK of 6.9 ± 0.1 is important for optimal acetyltransferase activity, determined from the best fit of the data to eq 3. As can be seen from the plateau-shaped pH profile in Figure 4A, the descending nature of the plot indicates that the ionizable group identified must be protonated for optimal catalytic efficiency. Since the determined pK value of 6.9 is consistent with the ionizable group of a histidine imidazole, pH studies were repeated with the His74Ala site mutant to investigate whether this residue was responsible for the observed pH dependence of wild-type AAC(6′)-Ii, the results of which are discussed below.

Steady-state kinetic parameters determined for the His74Ala mutant revealed only a small effect on enzyme activity. K_m values for acetyl-CoA and the 4,5- and 4,6-disubstituted aminoglycosides only differed by a range of 2−7.5-fold compared to that of the wild type, indicating no significant change in the apparent affinity (Table 2). Similarly, rates of acetyl transfer to the aminoglycosides that were tested were almost identical to those obtained for the wild-type protein. k_{cat}/K_m values were only slightly lower than that of the wild type, ranging from a 6-fold reduction in tobramycin acetylation efficiency to a 20-fold decrease observed for neamine (Table 2). Surprisingly, solvent viscosity effects indicated that this substitution altered the rate-determining step of acetyl transfer from a diffusion-controlled process to the chemical step. As can be seen from Table 3, no viscosity effect was observed for k_{cat}/K_b when aminoglycoside was the varied substrate, in contrast to the significant effect observed for the wild-type enzyme. Also supporting the importance of this residue are the results from pH studies with the His74Ala site mutant. Figure 4B clearly shows that the pH profile of His74Ala activity lacks the descending limb evident in the wild-type plot (Figure 4A), revealing that the ionizable group of this residue was identified from the wild-type pH profile. Most importantly, these findings support the identification of the ionization of the His74 imidazole, with a pK_a of 6.9 and in its protonated form, as being essential for optimal AAC(6′)-Ii activity, which effectively rules out the possibility that this residue functions as an active site base. The relative proximity of the His74 NE2 group to the carbonyl oxygen of acetyl-CoA (∼5 Å) in the crystal structure (Figure 3B) raises an interesting possibility that it may serve to polarize this oxygen for greater electrophilicity at the carbonyl carbon and also stabilize the negative charge which forms on the carbonyl oxygen in the transition state. His74 may therefore contribute to the formation of an oxyanion hole in the AAC(6′)-Ii active site.

Mutation of Leu76. The potential role of the main chain NH group of Leu76 in catalysis was investigated by mutating this residue to Ala or Pro, with the latter substitution eliminating the hydrogen bonding capacity of the backbone NH group. The Leu76Ala mutant demonstrated virtually wild-type activity as expected, with the biggest changes being a 3.6-fold reduction in the apparent affinity for neomycin and a 3.7-fold decrease in k_{cat} for amikacin (Table 2). Sucrose viscosity effects for this mutant were identical to those of the wild-type enzyme, indicating that diffusion-controlled processes still governed the rate of acetyl transfer (Table 3). In contrast, the Leu76Pro mutant was found to be dramatically impaired in both aminoglycoside recognition and catalysis. Specificity constants in particular revealed a large decrease in AAC(6′)-Ii catalytic efficiency, including a 2300-fold decrease in k_{cat}/K_b for neamine modification, a 1300-fold reduction in k_{cat}/K_b for tobramycin, and no detectable acetyl transfer activity toward several aminoglycosides (Table 2). Consistent with the kinetic analysis is the lack of a solvent viscosity effect on k_{cat}/K_b (Table 3), revealing that the substitution of Leu76 with Pro generates a catalytic mutant impaired at the chemical step. These results and the obvious differences in Leu76Ala and Leu76Pro protein activities lend support to a role for the backbone NH group of Leu76 in catalysis.

As Leu76 is adjacent to the GNAT-conserved β-bulge in AAC(6′)-Ii, mutation of this residue to Pro would result in two adjacent prolines along β-strand 4. We are confident, however, that the kinetic changes for this mutant are a result of functional alterations in AAC(6′)-Ii chemistry, as opposed to structural changes in the active site as a consequence of

the introduced mutation. First, wild-type proteolysis patterns were observed for the Leu76Pro mutant, indicating no gross changes in AAC(6′)-Ii tertiary structure. Also, the mutation to Pro is not expected to alter the hydrogen bonding patterns between β-strands 3 and 4, since the amide NH group of Leu76 does not participate in these interactions. Finally, the Leu76Pro site mutant displays only a marginal decrease (2-fold) in its affinity for acetyl-CoA, suggesting that this mutation does not affect the enzyme's interactions with this substrate. Taken together, the evidence presented here does implicate the amide NH group of Leu76 in transition-state or intermediate stabilization and reveals that this backbone interaction is a requirement for efficient AAC(6′)-Ii catalysis.

Role of Tyr147. Replacement of Tyr147 with Ala caused significant reductions in the affinity of AAC(6′)-Ii for all the aminoglycosides that were tested in addition to reductions in k_{cat} (Table 2). As a result, specificity constants (k_{cat}/K_m) were dramatically lower than for the wild-type protein, with changes ranging from 250-fold for ribostamycin acetylation to a greater than 3000-fold reduction for neamine modification. Characterization of the Tyr147Phe mutant was more informative, as the substitution with Phe maintains the aromatic ring of the side chain but removes the hydrogen bonding potential and general acid capabilities of the Tyr phenolic hydroxyl. As can be seen from Table 2, this mutant also demonstrated significant reductions in both the apparent affinity (K_m) and catalytic turnover (k_{cat}), resulting in specificity constants lower than that of the wild-type enzyme. In particular, decreases in aminoglycoside affinity ranged from a 6-fold decrease for tobramycin to a large 170-fold change in K_m for amikacin (Table 2). In general, the significant reductions in catalytic efficiency observed for the Tyr147Phe mutant suggest that the side chain hydroxyl plays a critical role in AAC(6′)-Ii catalysis. Solvent viscosity studies on both Tyr147Ala and Tyr147Ala proteins, however, demonstrated that rate-limiting segments in catalysis remained diffusion-controlled, with only slightly smaller effects observed for the Tyr147Ala mutant compared to the wild-type enzyme (Table 3). As well, pH studies did not identify an ionizable group consistent with a Tyr as being important for protein activity, suggesting that Tyr147 is not acting as an active site acid. The results presented here are consistent with the hydroxyl group of Tyr147 acting in some capacity to orient the acetyl moiety of acetyl-CoA for optimal interaction with aminoglycoside. It is possible that without this interaction the position of the acetyl group may be altered slightly and actually perturb the productive binding of aminoglycoside, likely explaining the reductions in Tyr147Phe affinity noted for this second substrate. Our results therefore suggest that Tyr147 does not act as the general acid in catalysis, but instead plays a major role in orienting the acetyl group for efficient transfer to the 6′-amino group of aminoglycosides.

MIC Determinations. To complement our *in vitro* analysis, we investigated the effects of each amino acid substitution on protein activity *in vivo* by determining the MIC values of kanamycin and neomycin for *E. coli* BL21(DE3) cells expressing either wild-type AAC(6′)-Ii or one of the site mutants. As can be seen from Table 4, all of the mutants conferred a lower level of resistance to kanamycin A compared to the wild-type protein. Increased susceptibility to this aminoglycoside was most notable with Leu76Pro, Tyr147Ala, and Tyr147Phe proteins, revealed by a 16-fold change in the MIC (Table 4). Similarly, the substitution of Glu72 with Ala caused an 8-fold change in the MIC with kanamycin A, likely due to the large decreases in protein affinity for aminoglycoside substrates as determined from our kinetic studies. In contrast to that observed for kanamycin A, changes in MICs in the presence of neomycin were for the most part small, with no change observed for the Leu76Ala mutant and only a 2-fold decrease in the MIC due to Glu72Ala, His74Ala, Tyr147Ala, and Tyr147Phe activities. The Leu76Pro protein, on the other hand, conferred no resistance to neomycin, with *E. coli* cells expressing this mutant becoming completely susceptible to this aminoglycoside (Table 4). Overall, the increase in drug susceptibility observed with a decrease in the MIC for *E. coli* cells expressing the mutant enzymes correlated well with changes in protein activity demonstrated *in vitro*.

Table 4: MICs of Select Aminoglycosides for AAC(6′)-Ii Site Mutants

	MIC (μg/mL)	
	kanamycin A	neomycin
BL21(DE3)[a]	4	1
wild type	128	8
Glu72Ala	16	4
His74Ala	32	4
Leu76Ala	32	8
Leu76Pro	8	1
Tyr147Ala	8	4
Tyr147Phe	8	4

[a] Negative control using *E. coli* BL21(DE3) and *E. coli* BL21(DE3)/pET22b(+).

Implications for the GNAT Superfamily. Characterization of the AAC(6′)-Ii site mutants described here has convincingly shown the importance of Glu72, His74, Tyr147, and the amide NH group of Leu76 in catalysis. Since the structural fold and active site geometry of GNAT enzymes are very similar, our results also allow us to compare the functions of these residues with equivalent amino acids from other GNAT enzymes. Our finding that Glu72 is not behaving as the active site base in AAC(6′)-Ii catalysis contrasts what was shown for Glu173 from tGCN5, an equivalent residue acting as the general base in histone modification (*34*). Similarly, His122 from AANAT (*28*) and Asp99 from AAC(6′)-Ie (*35*) are geometrically equivalent to His74 from AAC(6′)-Ii, and have both been shown to function as an active site base. Our results indicate that His74 is instead critical for optimal enzyme activity in its protonated form, and may contribute to the formation of an oxyanion hole in the active site. Additional differences were also observed for the role of the GNAT-conserved Tyr in acetyl transfer. Tyr168 from AANAT has been characterized as the general acid in serotonin acetylation by AANAT (*28*), with a similar function for AAC(6′)-Ii Tyr147 not supported by our results. Interestingly, mutation of an equivalent Tyr in AAC(6′)-Ib (Tyr166) and *in vivo* analysis of protein activity implicated this residue in the recognition of aminoglycoside substrates (*36*), which is consistent with the changes in aminoglycoside affinity that we observed with the mutation of Tyr147 in AAC(6′)-Ii. Last, we have shown the importance of the amide NH group of Leu76 in AAC(6′)-Ii activity, a finding that supports its involvement in transition-state or

intermediate stabilization and confirms previous speculation that this main chain element is critical for catalysis.

Our results, and the growing body of information available on the catalytic mechanisms of several other GNAT enzymes, clearly reveal differences in catalysis among these proteins, particularly in the function of geometrically equivalent, active site residues. As members of this superfamily are structural homologues and bind acetyl-CoA in a similar manner, we propose that the observed differences are a consequence of the acyl-accepting substrate. Since all GNAT enzymes to our knowledge follow a ternary complex mechanism, the requirement to bind both substrates in the active site would generate obvious differences in acetyl transfer chemistry, especially given the diverse group of acyl-accepting substrates. The unique ability of AAC(6′)-Ii to acetylate both aminoglycosides and basic proteins, for example, could be attributed to the different roles of active site residues as discussed, compared to other AACs and HAT enzymes. Furthermore, with the exception of the Leu76Pro mutation, mutagenesis of amino acid residues, while impeding optimal catalysis, did not result in catastrophic loss of activity either *in vivo* or *in vitro*. This parallels several studies with other GNAT family members. The primary role of the GNAT protein scaffold may then simply be to bind and orient acyl-CoAs and their cognate substrates in a geometry that is appropriate to acyl group transfer, rather than to provide a framework for setting an arrangement of amino acid residues that are essential for group transfer chemistry.

ACKNOWLEDGMENT

We thank Steve Radinovic for his help in mutagenesis and protein purification during his undergraduate project. We also thank Drs. Murray Junop and Quyan Hoang with technical assistance in generating Figure 3B.

SUPPORTING INFORMATION AVAILABLE

Partial proteolysis of AAC(6′)-Ii by subtilisin to assess the structural integrity of the mutant proteins relative to wild-type AAC(6′)-Ii and equilibrium dialysis and fluorescence anisotropy experiments performed to determine the dissociation constant (K_d) for acetyl-CoA and to investigate whether this value could be equated to the kinetic parameter K_m for this substrate. This material is available free of charge via the Internet at http://pubs.acs.org.

REFERENCES

1. Wright, G. D., Berghuis, A. M., and Mobashery, S. (1998) *Adv. Exp. Med. Biol. 456*, 27−69.
2. Davies, J., and Wright, G. D. (1997) *Trends Microbiol. 5*, 234−240.
3. Llano-Sotelo, B., Azucena, E. F., Kotra, L. P., Mobashery, S., and Chow, C. S. (2002) *Chem. Biol. 9*, 455−463.
4. Patterson, J. E., and Zervos, M. J. (1990) *Rev. Infect. Dis. 12*, 644−652.
5. Wennersten, C. B., and Moellering, R. C., Jr. (1980) in *Current Chemotherapy and Infectious Disease* (Nelson, J. D., and Grassi, C., Eds.) pp 710−712, American Society for Microbiology, Washington, DC.
6. Huycke, M. M., Sahm, D. F., and Gilmore, M. S. (1998) *Emerging Infect. Dis. 4*, 239−249.
7. Murray, B. E. (1998) *Emerging Infect. Dis. 4*, 37−47.
8. Shaw, K. J., and Wright, G. D. (2000) in *Gram-Positive Pathogens* (Fischetti, V. A., Novick, R. P., Ferretti, J. J., Portnoy, D. A., and Rood, J. I., Eds.) pp 635−646, American Society for Microbiology, Washington, DC.
9. Daigle, D. M., Hughes, D. W., and Wright, G. D. (1999) *Chem. Biol. 6*, 99−110.
10. Costa, Y., Galimand, M., Leclercq, R., Duval, J., and Courvalin, P. (1993) *Antimicrob. Agents Chemother. 37*, 1896−1903.
11. Wright, G. D., and Ladak, P. (1997) *Antimicrob. Agents Chemother. 41*, 956−960.
12. Draker, K. A., Northrop, D. B., and Wright, G. D. (2003) *Biochemistry 42*, 6565−6574.
13. Wybenga-Groot, L. E., Draker, K., Wright, G. D., and Berghuis, A. M. (1999) *Struct. Folding Des. 7*, 497−507.
14. Wolf, E., Vassilev, A., Makino, Y., Sali, A., Nakatani, Y., and Burley, S. K. (1998) *Cell 94*, 439−449.
15. Dutnall, R. N., Tafrov, S. T., Sternglanz, R., and Ramakrishnan, V. (1998) *Cell 94*, 427−438.
16. Peneff, C., Mengin-Lecreulx, D., and Bourne, Y. (2001) *J. Biol. Chem. 276*, 16328−16334.
17. Vetting, M. W., Hegde, S. S., Javid-Majd, F., Blanchard, J. S., and Roderick, S. L. (2002) *Nat. Struct. Biol. 9*, 653−658.
18. Hickman, A. B., Namboodiri, M. A., Klein, D. C., and Dyda, F. (1999) *Cell 97*, 361−369.
19. Hickman, A. B., Klein, D. C., and Dyda, F. (1999) *Mol. Cell 3*, 23−32.
20. Angus-Hill, M. L., Dutnall, R. N., Tafrov, S. T., Sternglanz, R., and Ramakrishnan, V. (1999) *J. Mol. Biol. 294*, 1311−1325.
21. Clements, A., Rojas, J. R., Trievel, R. C., Wang, L., Berger, S. L., and Marmorstein, R. (1999) *EMBO J. 18*, 3521−3532.
22. Poux, A. N., Cebrat, M., Kim, C. M., Cole, P. A., and Marmorstein, R. (2002) *Proc. Natl. Acad. Sci. U.S.A. 99*, 14065−14070.
23. Rojas, J. R., Trievel, R. C., Zhou, J., Mo, Y., Li, X., Berger, S. L., Allis, C. D., and Marmorstein, R. (1999) *Nature 401*, 93−98.
24. Bhatnagar, R. S., Futterer, K., Farazi, T. A., Korolev, S., Murray, C. L., Jackson-Machelski, E., Gokel, G. W., Gordon, J. I., and Waksman, G. (1998) *Nat. Struct. Biol. 5*, 1091−1097.
25. Weston, S. A., Camble, R., Colls, J., Rosenbrock, G., Taylor, I., Egerton, M., Tucker, A. D., Tunnicliffe, A., Mistry, A., Mancia, F., de la Fortelle, E., Irwin, J., Bricogne, G., and Pauptit, R. A. (1998) *Nat. Struct. Biol. 5*, 213−221.
26. Dyda, F., Klein, D. C., and Hickman, A. B. (2000) *Annu. Rev. Biophys. Biomol. Struct. 29*, 81−103.
27. Trievel, R. C., Rojas, J. R., Sterner, D. E., Venkataramani, R. N., Wang, L., Zhou, J., Allis, C. D., Berger, S. L., and Marmorstein, R. (1999) *Proc. Natl. Acad. Sci. U.S.A. 96*, 8931−8936.
28. Scheibner, K. A., De Angelis, J., Burley, S. K., and Cole, P. A. (2002) *J. Biol. Chem. 277*, 18118−18126.
29. Williams, J. W., and Northrop, D. B. (1978) *J. Biol. Chem. 253*, 5902−5907.
30. Leatherbarrow, R. J. (2000) *Grafit*, version 4.0, Erithacus Software, Staines, U.K.
31. Brannan, T., Althoff, B., Jacobs, L., Norby, J., and S., R. (2000) *Sigma Plot*, SSPS Inc., Chicago.
32. National Committee for Clinical Laboratory Standards (2000) Document M7-A5, Villanova, PA.
33. Cleland, W. W. (1986) in *Investigation of rates and mechanisms of reactions, part 1: general considerations and reactions at conventional rates* (Bernasconi, C. F., and Weisberger, A., Eds.) pp 854−870, John Wiley & Sons, New York.
34. Tanner, K. G., Trievel, R. C., Kuo, M. H., Howard, R. M., Berger, S. L., Allis, C. D., Marmorstein, R., and Denu, J. M. (1999) *J. Biol. Chem. 274*, 18157−18160.
35. Boehr, D. D., Jenkins, S. I., and Wright, G. D. (2003) *J. Biol. Chem. 278*, 12873−12880.
36. Shmara, A., Weinsetel, N., Dery, K. J., Chavideh, R., and Tolmasky, M. E. (2001) *Antimicrob. Agents Chemother. 45*, 3287−3292.
37. Kraulis, P. J. (1991) *J. Appl. Crystallogr. 24*, 946−950.
38. Merritt, E. A., and Murphy, M. E. P. (1994) *Acta Crystallogr. D50*, 869−873.
39. Gibrat, J. F., Madej, T., and Bryant, S. H. (1996) *Curr. Opin. Struct. Biol. 6*, 377−385.
40. Madej, T., Gibrat, J. F., and Bryant, S. H. (1995) *Proteins 23*, 356−369.
41. Richards, J. P., Bachinger, H. P., Goodman, R. H., and Brennan, R. G. (1996) *J. Biol. Chem. 271*, 13716−13723.

BI035667N